Atlantic Sea Surface Temperatures and Tropical Cyclone Formation

LLOYD J. SHAPIRO AND STANLEY B. GOLDENBERG

Hurricane Research Division, AOML/NOAA, Miami, Florida

(Manuscript received 17 July 1996, in final form 11 July 1997)

ABSTRACT

It has long been accepted that interannual fluctuations in sea surface temperature (SST) in the Atlantic are associated with fluctuations in seasonal Atlantic basin tropical cyclone frequency. To isolate the physical mechanism responsible for this relationship, a singular value decomposition (SVD) is used to establish the dominant covarying modes of tropospheric wind shear and SST as well as horizontal SST gradients. The dominant SVD mode of covarying vertical shear and SST gradients, which comprises equatorially confined near-zonal vertical wind shear fluctuations across the Atlantic basin, is highly correlated with both equatorial eastern Pacific SST anomalies (associated with El Niño) and West African Sahel rainfall. While this mode is strongly related to tropical storm, hurricanes, and major hurricane frequency in the Atlantic, it is not associated with any appreciable Atlantic SST signal.

By contrast, the second SVD mode of covarying vertical shear and horizontal SST gradient variability, which is effectively uncorrelated with the dominant mode, is associated with SST fluctuations concentrated in the main tropical cyclone development region between 10° and 20°N. This mode is significantly correlated with tropical storm and hurricane frequency but not with major hurricane frequency. Statistical tests confirm the robustness of the mode, and lag correlations and physical reasoning demonstrate that the SST anomalies are not due to the developing tropical cyclones themselves. Anomalies of SST and vertical shear during years where the mode has substantial amplitude confirm the resemblance of the individual fields to the modal structure, as well as the association of hurricane development with the warmer SSTs. Although SSTs are of secondary importance to vertical shear in modulating hurricane formation, explaining only ~10% of the interannual variability in hurricane frequency over the ~50% explained by vertical shear, the results support the conclusion that warmer SSTs directly enhance development. The lack of correlation with major hurricanes implies that the underlying SSTs are not a significant factor in the development of these stronger systems.

1. Introduction

Based upon thermodynamic arguments, it has long been accepted that some of the changes in tropical cyclone activity on interannual and interdecadal timescales are associated with fluctuations in the underlying sea surface temperature (SST). Work by Carlson (1971), Shapiro (1982), and Raper (1993) have attempted to quantify these relationships. Whether the fluctuations in SST are a direct cause of the observed changes in tropical cyclone development or are indirect indicators of other climatic fluctuations that themselves influence development has not, however, been established. As is well known, hurricanes rarely form when the underlying SST is below a threshold value of about 26.5°C (Palmén 1948; Gray 1968). The top panel of Fig. 1 shows the climatological SSTs[1] in the Atlantic basin during 1968–92 averaged for August–October (ASO), the ''peak'' months of the hurricane season when most hurricanes form. During ASO the climatological SSTs are above the 26.5°C threshold over the substantial part of the tropical and subtropical North Atlantic basin. Figure 2 shows the development locations of all ASO hurricanes in the Atlantic basin during 1968–92. Hurricanes are tropical cyclones with maximum sustained surface wind 33 m s^{-1} or more, while tropical storms have winds 18–32 m s^{-1}. Hurricanes that have attained a maximum sustained surface wind of 50 m s^{-1} are referred to as major (or intense) hurricanes. Of the 133 systems that later became hurricanes during the period, 63 (47%) initially reached depression strength between 9° and 20°N. In the recent paper by Goldenberg and Shapiro (1996) this band from ~10° to 20°N between the west coast of Africa and Central America was termed the ''main development region'' (MDR). Although the concentration of prehurricane depressions in this region is not as great as in Goldenberg and Shapiro (1996), where only precursors to major hurricanes were included, this

Corresponding author address: Dr. Lloyd Shapiro, Department of Atmospheric Sciences, Colorado State University, Fort Collins, CO 80523. E-mail: shapiro@chandra.atmos.colostate.edu

[1] The SSTs in this study are obtained from analyses provided by the Geophysical Fluid Dynamics Laboratory (GFDL) of the National Oceanic and Atmospheric Administration (NOAA), as described by Oort et al. (1987).

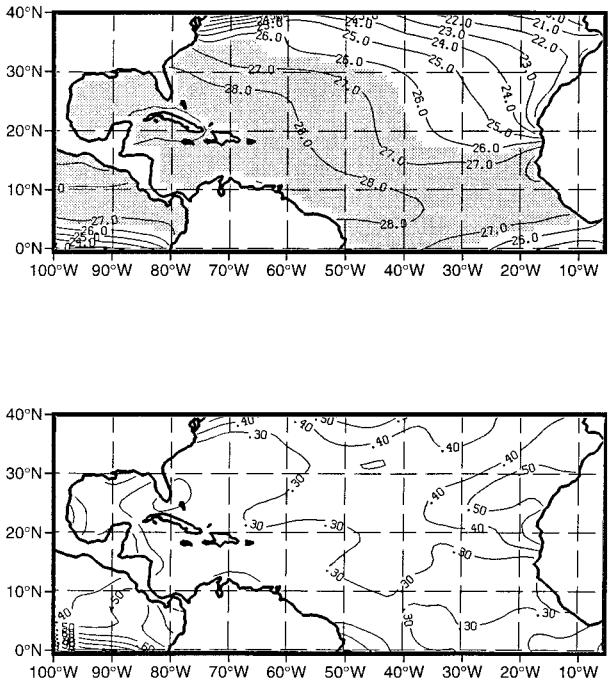

FIG. 1. Climatological SSTs for ASO of 1968–82 (top panel; contour interval 1°C) and standard deviations (bottom panel; contour interval 0.1°C). SSTs above the 26.5°C threshold are shaded.

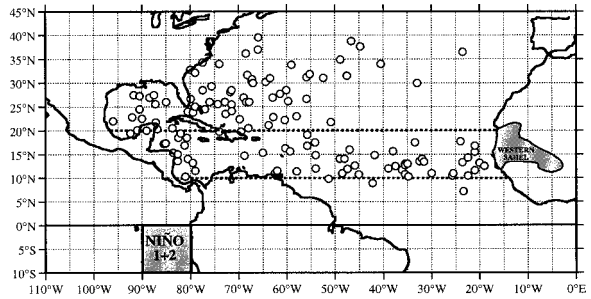

FIG. 2. Locations (open circles) where systems that became hurricanes during ASO of 1968–92 initially achieved a closed surface circulation (depression strength). The Niño 1 + 2 regions used to derive the El Niño index and the region in the western Sahel that contains the rainfall stations used by Landsea and Gray (1992) to derive the Sahelian rainfall index are also indicated (see section 2b). Dashed lines delineate northern and southern boundaries of main development region (see text).

terminology will be retained here. Systems that develop in the MDR are almost exclusively of easterly wave origin, while many of the systems that develop to the north of 25°N, particularly north of the 26°C isotherm in the top panel of Fig. 1, are of baroclinic origin (e.g., Frank 1970).

As shown in the bottom panel of Fig. 1, the fluctuations in seasonally averaged SST are only ~0.3°C in the MDR. The correlation (r) between Atlantic basin ASO hurricane frequency and May–July (MJJ) SST anomalies[2] is shown in the top panel of Fig. 3. The shaded regions indicate correlations that are significant using an a priori F-test at the 95% level (Kleinbaum and Kupper 1978).[3] These correlations are similar to those presented by Raper (1993) for a longer record. Though the correlations indicate that warmer SSTs precede seasons during which hurricane frequency is greater, as was also found by Shapiro (1982), the spatial extent of the significant regions is very small. The concentration of the significant correlations to the north of the MDR led Raper (1993) to suggest that the observed correlations are not a direct result of higher Atlantic SSTs themselves influencing hurricane formation, but rather an indication of an indirect relationship due to large-scale circulation features that influence both SSTs and hurricanes. Since oceanic upwelling and mixing due to a hurricane tend to cool the SST (see chapter 6 of Anthes 1982), it is quite unlikely that positive corre-

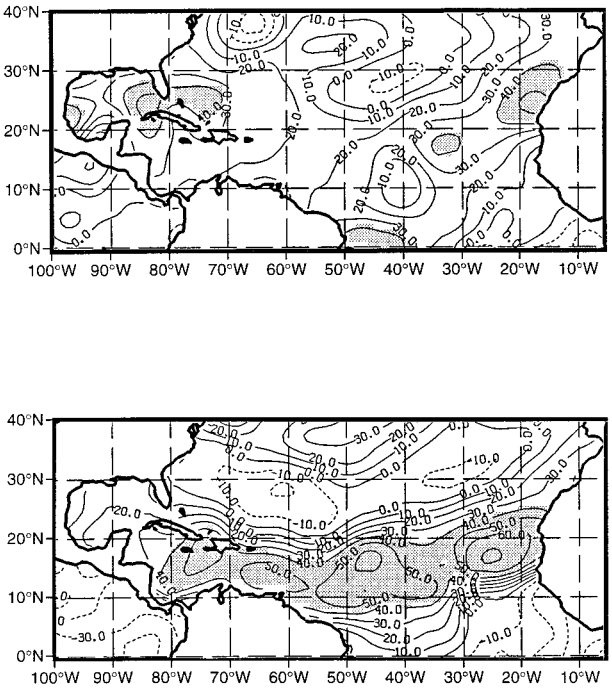

FIG. 3. Correlation between ASO Atlantic basin hurricane frequency and MJJ SSTs (top panel) as well as ASO SSTs (bottom panel). Magnitudes are multiplied by 100; contour interval is 0.1. Negative contours are dashed. Regions where the correlations are significant at the 95% level are shaded.

[2] All times series in the present paper are for the period 1968–92 and have been detrended prior to correlations being computed.

[3] Throughout this paper statistical significance is based on degrees of freedom derived from a sample size of 25, assuming that the individual years are statistically independent. A classic runs test for serial correlation [Siegel (1956) and footnote on p. 1382 of Shapiro (1984)] confirms that the series of tropical storm, hurricane, and major hurricane frequency (see below), as well as indices of El Niño and Sahel rainfall (see section 2b), are nearly random.

lations between hurricane frequency and SSTs are due to the hurricanes themselves. The use of MJJ SSTs to predict ASO hurricane frequency avoids questions of causality even more, since the correlations could not be due to the developing hurricanes.[4] To evaluate the direct effect of SSTs on hurricane frequency, however, contemporaneous correlations are required. The bottom panel of Fig. 3 evidences a substantial region of statistically significant positive correlations between hurricane frequency and ASO SST anomalies in the MDR, indicating that warmer SSTs coincide with greater hurricane frequency. Reductions of variance (r^2) as large as 0.5 appear. These correlations imply that underlying SSTs may have a direct influence on the development of the hurricanes, presumably by providing a more or less favorable thermodynamic environment for intensification of weaker systems.

Previous studies have established a strong relationship between seasonal Atlantic hurricane activity and both West African Sahel rainfall (Gray 1990; Landsea and Gray 1992) and eastern equatorial Pacific SST anomalies associated with El Niño (Gray 1984; Shapiro 1987). Warmer SSTs in the equatorial eastern Pacific are associated with reduced Atlantic basin hurricane activity. The correlations between a measure of El Niño (see section 2b) and Atlantic SSTs (not shown) are, however, much too weak and of the wrong sign to explain the observed correlations between Atlantic SSTs and hurricanes (Fig. 3). Above-normal western Sahelian monsoon rainfall is associated with increased Atlantic hurricane activity. The well-established relationship between Sahel rainfall and Atlantic SST anomalies (e.g., Folland et al. 1991), however, also cannot explain the observed correlations between hurricanes and Atlantic SSTs. Although greater rainfall is associated with warmer SSTs in the North Atlantic, partial correlations (not shown) confirm that the Atlantic SST anomalies associated with a measure of Sahel rainfall (see section 2b) are too weak and too localized near the coast of Africa to explain the observed correlations between Atlantic SSTs and hurricanes.

Previous studies have also established that fluctuations in the magnitude of the tropospheric vertical wind shear are one of the most important factors associated with changes in seasonal hurricane frequency (Gray 1984; Shapiro 1987). As recently shown by Goldenberg and Shapiro (1996), relationships between Atlantic major hurricane frequency and equatorial eastern Pacific SST anomalies as well as West African Sahel rainfall are explained primarily by their associations with vertical shear over the MDR. Figure 4 shows the vector correlation between ASO hurricane activity and vertical shear. To derive as long a record as possible, the vertical shear is defined as the difference between the 200- and 700-mb winds.[5] As discussed in Shapiro (1987) and Goldenberg and Shapiro (1996), increased hurricane activity is associated with an equatorially confined near-zonal circulation with upper-level easterly and lower-level westerly anomalies that act to decrease the magnitude of the climatological westerly vertical shear in the MDR. Below-normal activity, on the other hand, is associated with a circulation of the opposite sense that increases the vertical shear.

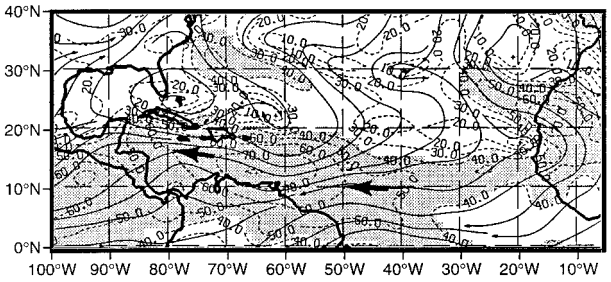

FIG. 4. Correlation between ASO hurricane activity and vertical shear. Dashed contours indicate multiple correlation coefficient based on both wind components (magnitudes ×100; contour interval 0.1). Streamlines are in the direction of the vector given by the correlations with the individual components. Regions where the correlations are significant at the 95% level (based on a single variable and a liberal sample size of 25) are shaded.

The purpose of the present paper is to isolate the physical mechanism responsible for the contemporaneous association between Atlantic SSTs and tropical cyclone (tropical storm, hurricane, or major hurricane) frequency. To this end, in section 2 the covarying modes of Atlantic SST and vertical wind shear variability are first derived. It is found that the dominant mode, while capturing the large-scale SST variability, is not statistically related to hurricane frequency. Horizontal gradients of SST are then used in the analysis, in place of SST itself, in order to emphasize more local SST variations. The dominant mode is found to isolate basin-scale changes in vertical shear that are statistically related to El Niño and Sahel rainfall. The second mode, which is effectively independent of the first, isolates SST variations in the MDR and is significantly correlated with tropical storm and hurricane frequency. Correlations with the dominant modes support the conclusion that SST fluctuations have a direct influence on Atlantic tropical storm and hurricane frequency, though they are less important overall than vertical shear. Using individual years, section 3 supports the reality of the

[4] On average there are only about 0.5 hurricanes yr^{-1} occurring in MJJ during 1968–92, contrasting with 4.5 in ASO. Moreover, as noted in Shapiro (1982), the correlation between MJJ and ASO hurricanes is negligible and almost none of the MJJ hurricanes is present in the central Atlantic. Therefore, MJJ hurricanes should have very little influence on the correlations between MJJ SST and ASO hurricanes.

[5] The winds for ASO were derived from monthly mean analyses by the National Meteorological Center/NOAA obtained from the National Center for Atmospheric Research. Section 2b of Goldenberg and Shapiro (1996) has a further discussion of the analyses.

second mode and its relationship to hurricane development, and section 4 discusses the results.

2. Relationship to covarying SST gradients and vertical wind shear

a. Motivation

The method of singular value decomposition (SVD) has been developed to extract the dominant covarying (coupled) modes of variability between two fields (Prohaska 1976; Bretherton et al. 1992). The SVD technique is a generalization of empirical orthogonal function (EOF) analysis (Lorenz 1956; Davis 1976). Rather than extracting the modes that explain the greatest variance in a single field, as in EOFs, the SVD technique finds the covarying modes that explain the greatest covariance between fields. By using SVDs to relate variations in SST and vertical shear in an a priori manner, problems related to a posteriori selection are avoided. And as we will see later, the structure of the dominant SVD modes are themselves useful in physical interpretation of the relationships between hurricane activity and large-scale climatic fluctuations. Bretherton et al. (1992) contains a concise description of SVD analysis. Appendix A summarizes salient features and terminology gleaned from Bretherton et al. (1992); for further details on this and other related methods the reader is referred to that paper. As in Wallace et al. (1992), each time series is normalized prior to the SVD analysis. In the case of the scalar SST field the normalization is by the standard deviation of the respective series; in the case of the vector field of vertical shear the appropriate normalization is by the square root of the 2×2 variance tensor (Ooyama 1987; Shapiro 1986). The SVDs are derived from analyses sampled at 3° lat–long intervals.

The dominant SVD mode of covarying ASO SST and ASO vertical wind shear ($\mathbf{V}_z$) variability, shown as homogeneous correlation patterns (see appendix A) in Fig. 5, explains 51% of the squared covariance between the fields. The SVD is derived from SST and vertical shears south of ~30°N,[6] where 83% of the depressions that become hurricanes (including almost all those of easterly wave origin) form (see Fig. 2); the correlations are displayed over a less restricted domain. The temporal correlation between the expansion coefficients of the SST and $\mathbf{V}_z$ fields associated with this mode (see appendix A) is 0.87, which is significant at the 95% significance level using a Monte Carlo technique that randomly reorders the fields in time. This method, which was used by Wallace et al. (1992; see their section 4), is liberal because it does not account for the serial correlation associated with low-frequency climate signals that may substantially reduce the effective number of degrees of freedom in a series (e.g., Davis 1977; Chelton 1983). An additional test that does not suffer from this deficiency, and which was also used by Wallace et al. (1992), is applied in the next section.

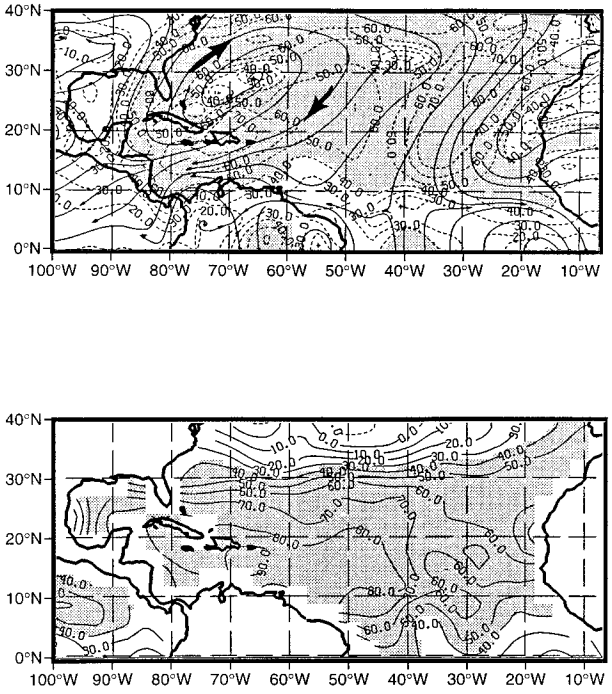

FIG. 5. Dominant SVD mode of covarying ASO SST and vertical wind shear variability. Homogeneous correlations are shown (see appendix A). Vertical shear pattern (top panel) is shown as vector correlations displayed as in Fig. 4. SST pattern (bottom panel) is shown also with significant correlations shaded.

The structure of the SST pattern of the dominant SVD (bottom panel of Fig. 5) evidences positive anomalies throughout almost the entire Atlantic basin, with statistically significant values covering the entire region from 10° to 30°N. As confirmed by correlation, this structure is virtually the same as that of the dominant SST EOF (not shown). The dominance of this EOF mode in the SVD analysis may be due to the large fraction of the SST variance explained by the dominant SST EOF (Wallace et al. 1992). The corresponding $\mathbf{V}_z$ pattern (top panel of Fig. 5) has an anticyclonic circulation centered at about 30°N, 60°W. The position of the anticyclone, which has a magnitude of 1–2 m s^{-1}, is near the axis of the climatological tropical upper-tropospheric trough during ASO. When the anticyclone is stronger, the trough is weakened. The correlation between the expansion coefficients of this mode and Atlantic ASO hurricane frequency explains only ~12% of the variance, which is not statistically significant. Therefore this mode is not statistically related to hurricane frequency.

As shown in Fig. 3, the correlation between Atlantic ASO hurricane activity and ASO SSTs is localized in the main development region between 10° and 20°N. As noted above, however, the dominant SVD mode de-

[6] Excluding the eastern Pacific Ocean basin (see region presented in Fig. 6).

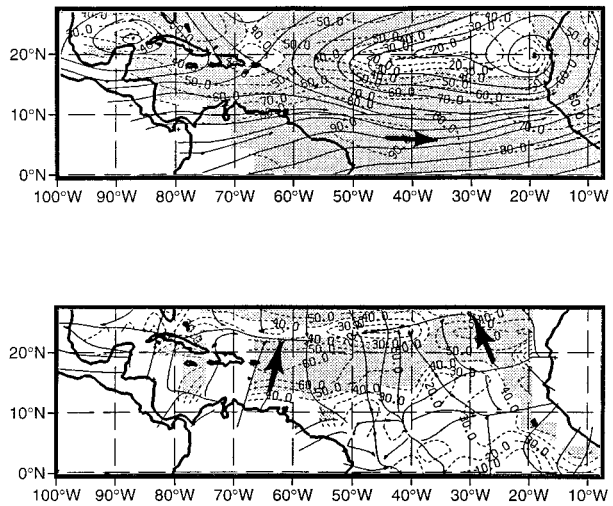

FIG. 6. Same as Fig. 5 but for dominant mode of covarying ASO horizontal SST gradients and vertical shear variability. Pattern of ∇SST (bottom panel) is shown as vector correlations as well.

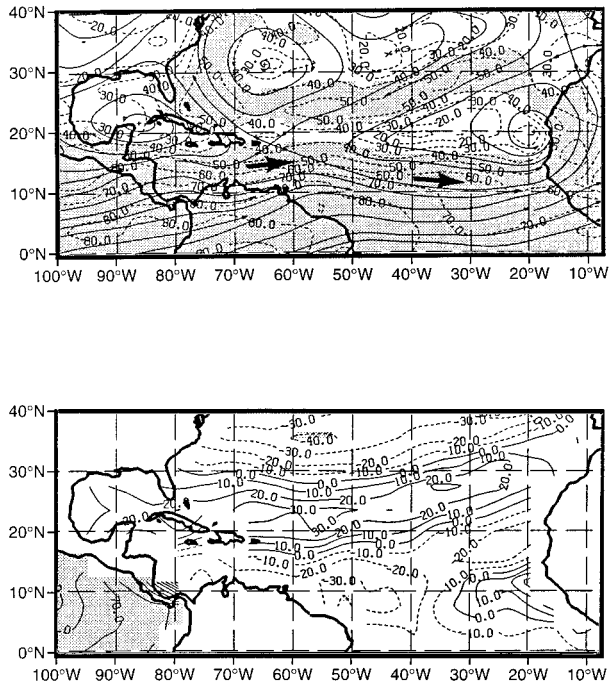

FIG. 7. Same as Fig. 6 but for heterogeneous correlations (see appendix A), with the top panel presenting the vector correlations between the $\mathbf{V}_z$ field and the expansion coefficient for ∇SST, and the bottom panel the correlations between the SST field and the expansion coefficient for $\mathbf{V}_z$.

scribing the covarying SST and vertical wind shear variability (Fig. 5) is determined by the dominant SST EOF. By its very nature the dominant SST EOF maximizes the total variance explained and thus tends to have a large-scale (global) structure. As a result, the dominant mode is not significantly correlated with hurricane frequency. To relate modes of covarying SST and $\mathbf{V}_z$ variability to hurricanes, a methodology that emphasizes more local SST variations must be utilized. The method of ''rotating'' EOFs has been used to considerable advantage in isolating the ''simple'' (local) variations in a field (e.g., Horel 1981). By relaxing the orthogonality constraint, the rotated modes tend to be less dependent on the domain geometry than are EOFs, have less sampling variability, and show a stronger resemblance to individual fields (Richman 1986).[7] As a simple alternative to rotation, in the present section we will use horizontal gradients of SST to accentuate the local character of the variations in the SST field.[8] With this methodology an SVD analysis can be used to isolate the significant covarying SST and vertical wind shear variations that are strongly related to tropical cyclone frequency. It might be expected that the vertical wind shear would be in thermal wind balance with the underlying horizontal gradients of SST. The significant covarying modes, derived in sections 2b and 2c, do not, however, themselves evidence a structure that is consistent with such a simple balance. Nevertheless, these modes are able to resolve two distinct physical mechanisms. The methodology allows basin-scale $\mathbf{V}_z$ variations, which are known to be strongly related to hurricane development, to dominate the first (dominant) mode. The second mode, which is effectively independent of the first, then isolates SST variations in the MDR.

b. Dominant mode

The dominant SVD mode of covarying ASO horizontal SST gradient (∇SST) and ASO $\mathbf{V}_z$ variability is shown in Fig. 6 over the region used to derive the mode. This mode explains 26% of the squared covariance between the fields. The correlation between the expansion coefficients for this mode is 0.93, which is significant by the same Monte Carlo test used in the previous section. Since ∇SST is a vector, the corresponding homogeneous correlations are presented in vector form. Although the ∇SST distribution evidences northward gradients concentrated near 20°N, it is difficult to interpret the pattern in terms of SST itself.

An alternate depiction of the dominant mode is given in Fig. 7, which presents heteorogeneous correlations (see appendix A) over the extended domain. The top

[7] Very recently, Cheng and Dunkerton (1995) have presented a method for rotating SVDs. This methodology was not available when the present study was made. As with EOFs, the SVD rotation methodology requires subjective judgments as to the criterion for simplicity as well as the number of modes to rotate. The success of the technique used in the present study leads us to believe that reanalysis using rotation would not likely change the conclusions.

[8] If the SST field has a power spectrum $S(k)$ as a function of horizontal wavenumber, k, then the horizontal gradient of SST has spectrum $k^2S(k)$. Thus, small-scale (large k) components are enhanced.

TABLE 1. Reduction of variance (r^2) due to relationship with expansion coefficients of dominant and second SVD mode of covarying ∇SST and $\mathbf{V}_z$ variability. Relationships with numbers of tropical storms, hurricanes, and major hurricanes [adjusted for bias as in Landsea (1993)] that formed during ASO of 1968–92 are given. Relationships with the El Niño index (ENI) and the Sahel index (SI) are also given. Double asterisks (**) indicate correlations (r) significant at the 95% level.

	Dominant mode		Second mode	
	$a_1^{\mathbf{V}_z}$	$a_1^{\nabla\text{SST}}$	$a_2^{\mathbf{V}_z}$	$a_2^{\nabla\text{SST}}$
Tropical storms	0.24**	0.19**	0.21**	0.28**
Hurricanes	0.29**	0.24**	0.22**	0.29**
Major hurricanes	0.42**	0.38**	0.03	0.05
ENI	0.52**	0.36**	0.01	0.01
SI	0.38**	0.42**	0.06	0.06

panel presents the standard heterogeneous correlations, $r(\mathbf{V}_z, a_1^{\nabla\text{SST}})$, the correlations between the $\mathbf{V}_z$ field and the expansion coefficient for ∇SST. The vertical shear pattern evidences an equatorially confined westerly shear across the entire domain south of 20°N. It resembles the shear patterns that are associated with positive SST anomalies (associated with El Niño conditions) in the equatorial eastern Pacific (Shapiro 1987; Goldenberg and Shapiro 1996) and negative rainfall anomalies (associated with drought conditions) in the western Africa Sahel region (Goldenberg and Shapiro 1996). Correlations confirm that the vertical shear pattern is nearly the same as that of the dominant $\mathbf{V}_z$ EOF (not shown). The relationship with the Pacific SSTs can be quantified by using an El Niño index (ENI) defined as the mean SST for ASO over the Climate Prediction Center's Niño 1 + 2 region (see Fig. 2).[9] The correlation between ENI and the $\mathbf{V}_z$ expansion coefficient of the dominant mode explains 52% of the variance (Table 1), which is statistically significant. Similarly, the relationship with West African Sahelian rainfall can be quantified by using the Sahel index (SI) derived for June–September by Landsea and Gray (1992) (see Fig. 2), as also discussed by Goldenberg and Shapiro (1996; their section 2d). The correlation between SI and the $\mathbf{V}_z$ expansion coefficient of the dominant mode explains 38% of the variance (Table 1), which is also statistically significant. Therefore, as was apparent from the spatial pattern of the mode, the $\mathbf{V}_z$ anomalies are strongly correlated with both El Niño and West African rainfall. This mode will thus be referred to as the El Niño–Sahel index (ENSI) mode. The bottom panel, on the other hand, presents $r(\text{SST}, a_1^{\mathbf{V}_z})$, the correlations between the SSTs themselves and the expansion coefficient for $\mathbf{V}_z$. These correlations give a direct depiction of the SST distribution that it associated with this mode. Though the SST gradients associated with this mode (Fig. 6) are statistically significant near 20°N, the SST anomalies in the Atlantic basin associated with this mode are very small and not statistically significant.[10] Table 1 also presents the variances in ASO tropical storm, hurricane, and major hurricane frequency explained by the expansion coefficients for this mode. The correlations are all statistically significant, indicating the strong relationship between vertical shear anomalies in the main development region and hurricane activity discussed in section 1. Westerly $\mathbf{V}_z$ anomalies act to increase the magnitude of the vertical shear, thereby inhibiting hurricane development; easterly anomalies have the opposite effect (cf. Fig. 6 of Goldenberg and Shapiro 1996).

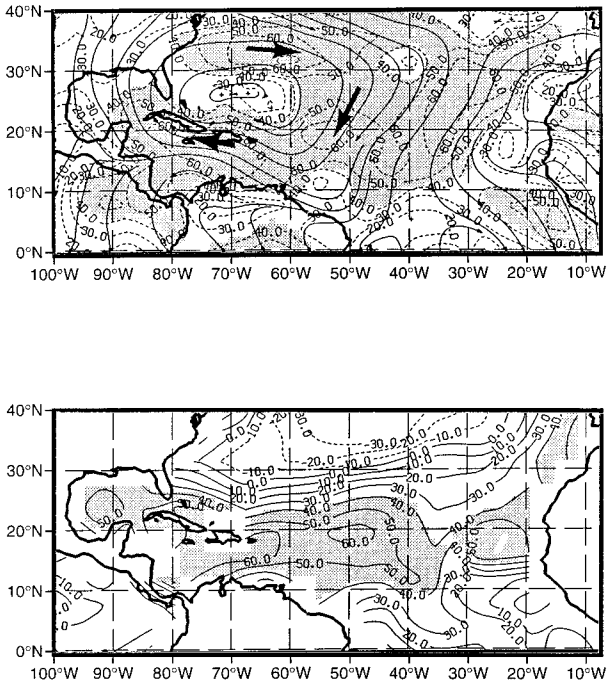

FIG. 8. Same as Fig. 7 but for second SVD mode of covarying ASO horizontal SST gradients and vertical shear variability.

c. Second mode

The second SVD mode of covarying ASO ∇SST and ASO $\mathbf{V}_z$ variability is shown in Fig. 8, using the same presentation as that in Fig. 7. This mode explains 15% of the squared covariance between the fields. The correlation between the expansion coefficients for this mode is 0.93, which is significant by the Monte Carlo test. The SST correlation pattern associated with this mode (bottom panel) evidences statistically significant positive anomalies that are concentrated in the MDR

[9] Before 1980 the values of ENI are the same as those derived by Goldenberg and Shapiro (1996; their section 2c). After 1979 the values differ slightly due to the present use of an updated GFDL dataset.

[10] The strong correlations in the eastern Pacific are consistent with the strong association between the expansion coefficient for this mode and the ENI.

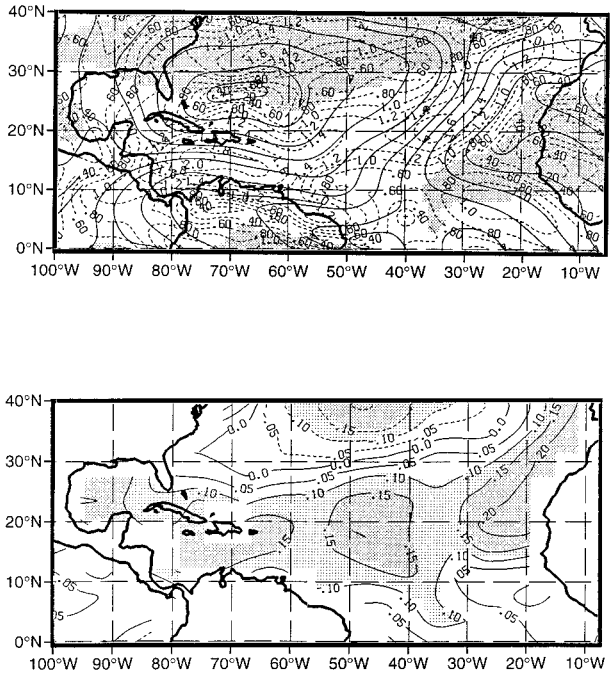

FIG. 9. Covariances between expansion coefficients of the second dominant mode of covarying ∇SST and $\mathbf{V}_z$ variability and $\mathbf{V}_z$ (top panel) as well as SST (bottom panel). Vertical shear contour interval is 0.2 m s^{-1}, with positive anomalies in the magnitude of the shear shaded. SST contour interval is 0.05°C, with negative values dashed and magnitudes greater than 0.10°C shaded.

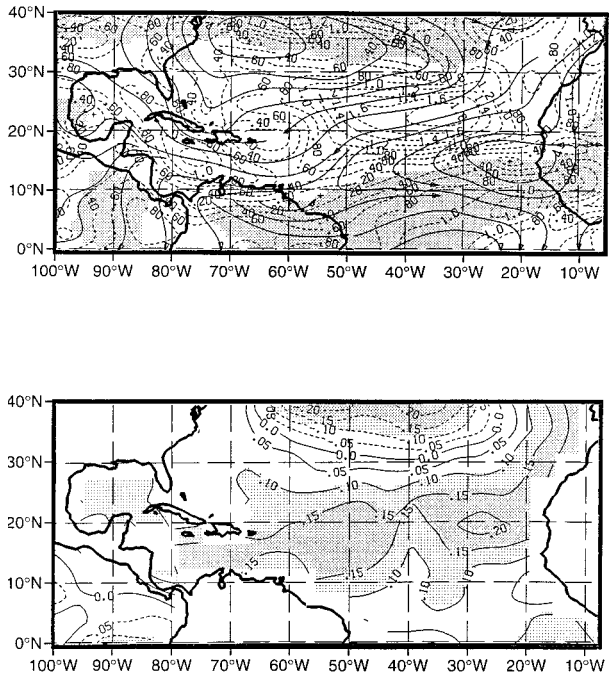

FIG. 10. Same as Fig. 9 but for covariances between expansion coefficients of the second dominant mode of covarying ∇SST and $\mathbf{V}_z$ variability and MJJ $\mathbf{V}_z$ (top panel) as well as MJJ SST (bottom panel).

between 10° and 20°N. The corresponding vertical shear correlation pattern (top panel) has an anticyclonic anomaly centered near 25°N, which is near the axis of the climatological tropical upper-tropospheric trough during ASO. The strong meridional component in the vertical shear evident in Fig. 8 contrasts with the near-zonal shear in the dominant mode (Fig. 7).

The resemblance between the SST pattern associated with the second SVD mode (bottom panel of Fig. 8) and the contemporaneous correlations between Atlantic SSTs and hurricane frequency (bottom panel of Fig. 3) implies that the SST anomalies associated with this mode may be related to hurricane development. Table 1 indicates that the expansion coefficients for this mode in fact explain about 25% of the variance in both hurricane and tropical storm frequency, a statistically significant relationship. The relationships with ∇SST are stronger than those with $\mathbf{V}_z$. The correlation between the expansion coefficients for this mode and El Niño (ENI), Sahel rainfall (SI), and major hurricane activity, by contrast, are very small and not statistically significant. The second mode is effectively uncorrelated with the dominant (ENSI) mode, which represents the changes in vertical shear over the MDR that especially affect major hurricane frequency (Goldenberg and Shapiro 1996). As demonstrated in appendix B, using a method that is not dependent on the degree of serial correlation, the second mode is statistically robust. The reality of the mode and its relationship to hurricane development will be further established in section 3 using individual years.

Dimensional characteristics of the second mode are shown in Fig. 9, which displays covariances between the expansion coefficients and $\mathbf{V}_z$ as well as SST. The covariance, cov($\mathbf{V}_z$, $a_2^{\nabla\text{SST}}$), for example, shows the vertical shear anomalies that are associated with a ∇SST expansion coefficient one standard deviation above normal. The mode has SST anomalies ~0.15°C in the main tropical cyclone development region that are associated with anticyclonic shears ~1 m s^{-1}, with weakened shear in the main development region accompanying warmer SSTs. The shears are dominated by upper-level (200 mb) wind anomalies (not shown). Possible physical causes for the associated vertical shear and SST patterns that accompany this mode are discussed in section 4.

The SST and $\mathbf{V}_z$ anomalies associated with this mode may both have an effect on and be affected by tropical storms in the region. Since, as noted in section 1, SSTs are generally cooled by upwelling associated with tropical storms, it is likely that the warmer SSTs associated with this mode are not due to the developing cyclones themselves. Further support for this contention is found in lag relationships. The bottom panel of Fig. 10 shows the covariance between the expansion coefficient of $\mathbf{V}_z$ for the second mode and MJJ SSTs, the 3 months preceding the ASO period used to derive the mode. The covariances are very similar to those displayed in the bottom panel of Fig. 9, with anomalies ~0.15°C in the

main development region. Since the SST anomalies associated with the mode existed prior to the ASO period, they must be due to factors not directly associated with the hurricanes themselves. The top panel of Fig. 10 shows the covariance between the expansion coefficient of ∇SST and MJJ $\mathbf{V}_z$. Although the covariances evidence anticyclonic anomalies in the northwestern Atlantic, they are farther to the north and generally much weaker than those in the top panel of Fig. 9. Thus, the vertical shear anomalies associated with the second mode may be due in part to systems, including hurricanes, that are present during ASO. On the other hand, the easterly anomalies in the MDR between 10° and 20°N in the top panels of Figs. 9 and 10 are associated with reduced vertical shear magnitudes. These vertical shear anomalies associated with this mode may very likely influence the development of tropical systems.

Due to the uncertainty as to how much the vertical shear influences (or is influenced by) the developing hurricanes, and the indirect nature of the relationship between the SVD mode and SSTs, the estimate of the contribution of SSTs associated with this mode to hurricane development over that due to $\mathbf{V}_z$ is problematic. Our estimate starts with an evaluation of the contribution of $\mathbf{V}_z$ to interannual fluctuations in hurricane frequency. The first five $\mathbf{V}_z$ EOFs (not shown) explain approximately 60% of the variance in hurricane frequency. The addition of more EOFs does not significantly increase the skill (variance explained). After adjusting for the expected artificial skill due to random errors, the estimated true skill (Lorenz 1956; Chelton 1983) from $\mathbf{V}_z$ is 50% of the variance. Inclusion of the second SVD expansion coefficient for $\mathbf{V}_z$ or ∇SST, which indirectly contain information on the SSTs associated with the mode, increases the estimated true skill to close to 61%. The increase of 11% is an estimate of the contribution of SSTs associated with the mode to interannual fluctuations in hurricane frequency over that explained by $\mathbf{V}_z$. This value is significant at the 95% level. It is also consistent with estimates obtained from partial correlations based on the SST and $\mathbf{V}_z$ fields themselves (not shown).[11] Thus, interannual fluctuations in SST have a small but apparently significant role in determining hurricane frequency.

3. Individual years

In the previous section the relationships between the second SVD mode of covarying ∇SST and $\mathbf{V}_z$ variability in the Atlantic and tropical cyclone fluctuations were established. Given the statistical nature of the analysis, it is important to analyze individual years where the mode has substantial amplitude to confirm the resemblance of the individual fields to the modal structure, as well as the association of hurricane development with warmer SSTs. The expansion coefficient of ∇SST for the second SVD mode of covarying ∇SST and $\mathbf{V}_z$ variability ($a_2^{\nabla SST}$) is shown in Fig. 11, indirectly representing the fluctuations in SST associated with this mode. The largest amplitudes are for the years 1969, 1977, 1981, and 1990. The ASO vertical shear and SST anomalies for these years are shown in Fig. 12, together with the tracks for each year of ASO systems from the point that they became depressions. Table 2 presents a summary of ASO tropical storm, hurricane, and major hurricane frequency for each of these years, as well as measures of El Niño (ENI) and West African Sahelian rainfall (SI), together with climatological values.

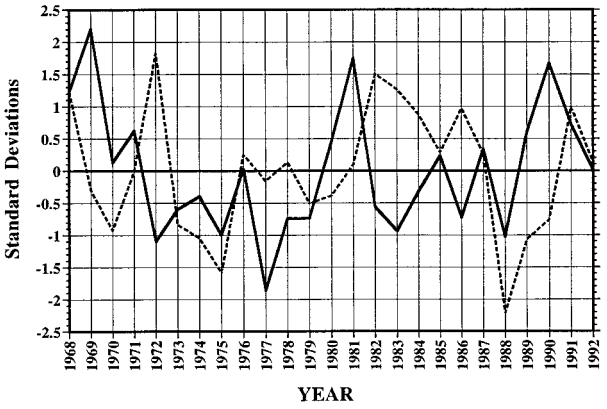

FIG. 11. Expansion coefficients of ∇SST for second SVD mode of covarying ∇SST and $\mathbf{V}_z$ variability (solid line), and of $\mathbf{V}_z$ for first SVD mode (dashed line). Values are given as standard deviations relative to a mean of zero.

The year 1969 was a very active year, with much greater than average tropical storm, hurricane, and major hurricane activity. While ENI was greater than normal, tending to suppress hurricane activity, SI was also above normal, tending to be associated with enhanced activity. The conflict between the two indices is resolved in an ENSI mode near normal, as indicated by the small value of the expansion coefficient $a_1^{\mathbf{V}_z}$, also shown in Fig. 11. The expansion coefficient $a_2^{\nabla SST}$, on the other hand, was more than two standard deviations above normal, implying warmer SSTs in the MDR (cf. SST structure of second mode in bottom panel of Fig. 8). Such SST anomalies are in fact seen for 1969 in Fig. 12a (bottom panel), with magnitudes ~0.5°C in some regions. The vertical shear anomalies evidence an anticyclone in the far western Atlantic centered near 25°N, also consistent with the structure of the second mode (top panel of Fig. 8). The tracks of the tropical storms indicate that development took place predominantly from systems that moved over anomalously warm water. These warm waters as well as the easterly shear anomalies in the MDR,

[11] In particular, SST anomalies in the MDR add about 10% to the variance of hurricane frequency over that explained by vertical shear in the MDR near 15°N, 65°W. By contrast, vertical shear near that location adds about 50% to the variance in hurricane frequency over that explained by SST in the main development region.

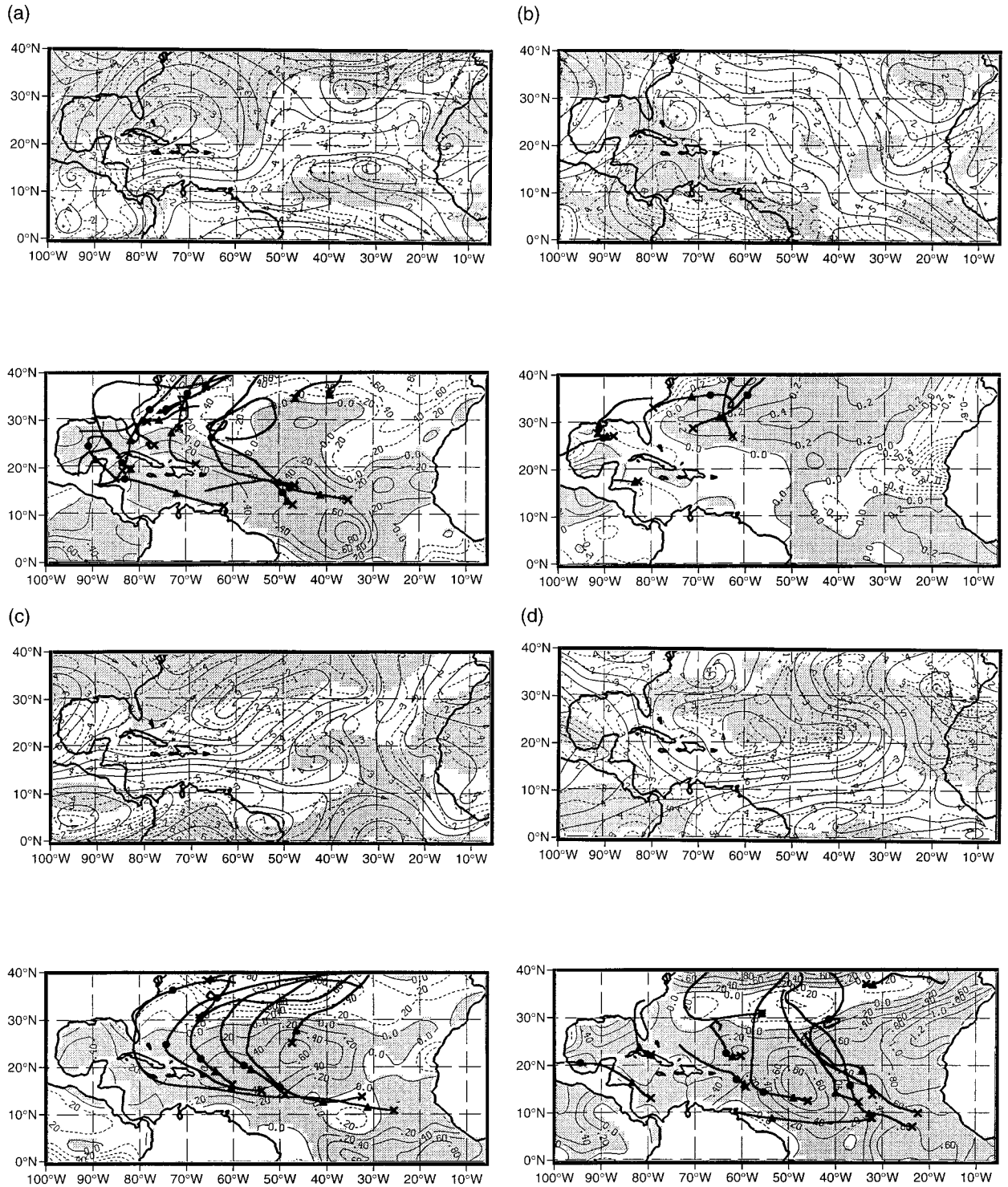

FIG. 12. Vertical shear anomalies (top panel; streamlines and isotachs in m s^{-1}) and SST anomalies (bottom panel; contour interval 0.2°C) during ASO for the years (a) 1969, (b) 1977, (c) 1981, and (d) 1990. Anomalies are with respect to 1968–92 climatology. Shading in the top panel indicates positive anomalies in the magnitude of the vertical shear. Bottom panel also displays tracks of all systems that developed into tropical storms during ASO of each year. Cross (×) represents the position that the system became a tropical depression, a solid triangle (▲) the position it became a tropical storm, and a solid circle (●) the position it became a hurricane.

TABLE 2. Numbers of tropical storms, hurricanes and major hurricanes [*adjusted for bias as in Landsea (1993)] that formed during ASO of years with greatest amplitude of $a_2^{\nabla SST}$ (see Fig. 11). ENI for ASO (relative to a 1950–79 climatology), and SI for June–September [given in mean standard deviations relative to 1949–90 average, as derived by Landsea and Gray (1992)] are also given. Average for 1968–92 is given in last column.

	1969	1977	1981	1990	Average
Tropical storms	15	6	8	13	7.4
Hurricanes	10	5	6	8	4.5
Major hurricanes	3*	1	3	1	1.6
ENI (°C)	0.7	−0.5	−0.5	−0.3	0.1
SI	0.6	−0.9	−0.3	−1.0	−0.5

and the associated reduced shear magnitudes, most likely contributed to increased hurricane activity.

The years 1977 and 1981 both had near-average tropical storm and hurricane activity, with the latter year having above-average major hurricane activity. While ENI was below normal for both years, SI was very dry in 1977 and near normal in 1981. The expansion coefficient $a_1^{\mathbf{V}z}$ was very small in both years, indicating near-neutral ENSI conditions. The expansion coefficient $a_2^{\nabla SST}$ was, however, about two standard deviations below normal in 1977 and two standard deviations above normal in 1981. Correspondingly, the actual SST anomaly in the main development region between 10° and 20°N was small or negative in 1977 (bottom panel of Fig. 12b) but positive in 1981 (bottom panel of Fig. 12c). While there was a broad anticyclonic anomaly in 1981 centered near 30°N in the western Atlantic (top panel of Fig. 12c), no such feature was present in 1977 (top panel of Fig. 12b). All of these features are consistent with the structure of the second mode (Fig. 8). The tracks of the tropical storms indicate clear differences between the two years as well. In each year development took place only where the SSTs were anomalously warm. In 1981 development was over the MDR; in 1977 it was mostly over the anomalously warm water to the north of 25°N.

As a last example, Fig. 12d shows the anomalies for 1990, a year with much greater than average tropical storm and hurricane activity but below average major hurricane activity. While ENI was slightly lower than normal SI was well below normal, indicating a very dry western Sahel and a tendency for suppressed hurricane (especially major hurricane) activity. The expansion coefficient $a_1^{\mathbf{V}z}$, on the other hand, was almost one standard deviation below normal, indicating favorable vertical shears for hurricane formation (consistent with ENI). The influence of these favorable shears was augmented by the warm SSTs in the entire region south of about 30°N, the breeding ground for almost all of the systems that became storms that year (bottom panel of Fig. 12d). The SST distribution as well as the vertical shears (top panel of Fig. 12d) are consistent with the structure of the second dominant mode (Fig. 8).

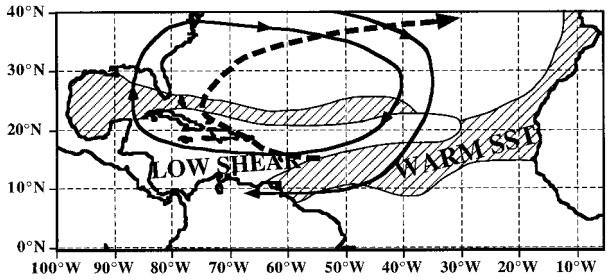

FIG. 13. Schematic of second SVD mode of covarying ∇SST and $\mathbf{V}_z$ variability, based on Figs. 8, corresponding correlations with the magnitude of the vertical shear (not shown), and Fig. 12. Warm SSTs (hatching) are associated with anticyclonic vertical shear anomalies (solid lines) that act to create low shear in the main development region (shading). A typical storm track is shown by the dashed line.

4. Discussion

The dominant SVD mode of covarying ∇SST and $\mathbf{V}_z$ variability in the Atlantic, termed the ENSI mode because of its high correlation with both an El Niño index (ENI) and a Sahelian rainfall index (SI), was presented in section 2b. It comprises equatorially confined near-zonal vertical wind shear fluctuations across the Atlantic basin. While this mode is strongly related to tropical storm, hurricane, and major hurricane frequency in the Atlantic, it is not associated with any appreciable Atlantic SST signal. By contrast, the second SVD mode of covarying ∇SST and $\mathbf{V}_z$ variability was shown in section 2c to be associated with SST fluctuations concentrated in the main tropical cyclone development region. This mode is significantly correlated with hurricane and tropical storm frequency but not with major hurricane frequency. Statistical tests confirmed the robustness of the mode, and physical reasoning as well as lag correlations demonstrated that the SST anomalies are not due to the developing tropical cyclones themselves. Anomalies of SST and $\mathbf{V}_z$ during years where the mode has substantial amplitude were presented in section 3, confirming the resemblance of the individual fields to the modal structure, as well as the association of hurricane development with anomalously warm SSTs in those years. Although the analyses themselves cannot unambiguously establish a direct causal link between the SST anomalies and hurricane formation, the results support the conclusion that warmer SSTs enhance development. The lack of correlation with major hurricanes implies that the underlying SSTs are not a significant factor in the formation of these stronger systems, which are very predominantly of easterly wave origin, probably because vertical shear in the main development region between 10° and 20°N dominates their development.

The character of the second SVD mode, and its relationship to hurricane development, is shown schematically in Fig. 13. Warmer SSTs are associated with a vertical shear anticyclone anomaly centered to their north, as well as greater hurricane activity. As noted in

section 2a, a simple thermal wind balance between horizontal surface temperature gradients and vertical shear cannot explain the association between the warmer SSTs and the vertical shear patterns that accompany this mode. It is possible in principle that a more indirect forcing of the atmosphere by the SSTs, through vertical motion and cloudiness patterns, for example, could explain the association. It is also possible that some part of the association could be due to oceanic forcing by low-level winds. The analysis of atmospheric variables besides horizontal winds as well as the oceanic response are beyond the scope of the present study. One other possible mechanism for the vertical shear–SST associations accompanying the second mode is related to the development of moving tropical systems. A tropical storm typically forms over the warmer waters and tracks to the northwest, tending to induce a warm-core structure with anticyclonic upper-tropospheric winds above a low-level cyclonic circulation. Therefore, as deduced in section 2c using lag correlations, part of the anticyclonic shear anomaly in Fig. 13 may be due to the developing storms themselves. The anticyclonic shear anomaly is associated with low shear in the main development region, itself favoring development. In section 2c it was estimated that SSTs associated with the mode explain only ~10% of the interannual variability in hurricane frequency over the ~50% explained by $\mathbf{V}_z$. Therefore SSTs are of secondary importance to fluctuations in hurricane formation. Nevertheless, since the SST anomalies are preexisting features in the region where the tropical storms typically develop (section 2c), the clear implication is that they have an active role in enhancing storm development. This conclusion contradicts that of Raper (1993).

The 1995 hurricane season was a very active year, with 15 tropical storms, 10 hurricanes, and five major hurricanes during ASO. The Sahel was dry, with SI = −0.5 (Landsea et al. 1997), equal to the 1968–92 mean, and thus basically neutral for storm development. By contrast, during ASO the eastern Pacific had cooler than normal SSTs, with ENI = −0.4°C (signifying a moderate La Niña event), and ASO vertical shear in the main development region between 10° and 20°N was correspondingly much below normal (Landsea et al. 1997). These factors were favorable for storm development. The Atlantic SST anomalies for the season were also quite favorable, being much above normal throughout the subtropics and the main development region (Landsea et al. 1997). While previous studies have well established that the reduced vertical shear could have contributed to the very active season, the present study implies that warmer SSTs probably played a role as well.

Acknowledgments. The authors thank Drs. Chris Landsea and Hugh Willoughby for their very helpful comments on an earlier version of this paper. Mr. Rodrigo Ortiz provided data processing assistance for some of the analyses.

APPENDIX A

SVD Analysis

As described by Bretherton et al. (1992), consider a time-dependent ''left'' data field, $s(\mathbf{x}, t)$, and a ''right'' data field, $w(\mathbf{y}, t)$, each representing anomalies (normalized as required) defined at N_s grid points $\mathbf{x}_i$ and N_w grid points $\mathbf{y}_i$, respectively, and at T observation times t. For simplicity we will consider both data fields to be scalars. Treatment of a vector field requires only a different normalization prior to analysis (see section 2a). In the present paper the left field (s) will either be the scalar SST or horizontal gradient vector ∇SST, while the right field (w) will be the vertical wind shear vector $\mathbf{V}_z$.

The data can be expanded in synthetic series,

$$\tilde{s}_N(\mathbf{x}, t) = \sum_{k=1}^{N} a_k^s(t) p_k(\mathbf{x})$$

$$\tilde{w}_N(\mathbf{y}, t) = \sum_{k=1}^{N} a_k^w(t) q_k(\mathbf{y}),$$

where the sum is over $N \leq \min(N_s, N_w)$ modes. The time series $a_k^s(t)$ and $a_k^w(t)$ are called ''expansion coefficients,'' and the vectors $p_k(\mathbf{x})$ and $q_k(\mathbf{y})$ are called ''patterns.'' The SVD patterns are spatially orthonormal. Each pair of coefficients and patterns together (for a given k) make up a ''mode.'' The coefficients and patterns are chosen so that the first mode maximizes $\langle a_1^s(t), a_1^w(t)\rangle$, the cross-covariance of the expansion coefficents, where the brackets denote the time average over the T observation times. Successive pairs explain the maximum covariance subject to orthogonality of the left and right patterns among themselves. The practical technique for computing the SVD modes in terms of eigensolutions of the cross-covariance matrix between the fields is presented in section 3a of Bretherton et al. (1992).

The homogeneous correlation map for the kth left field is defined as the linear correlation coefficient, $r[s(\mathbf{x}, t), a_k^s(t)]$, between the left field and the kth expansion coefficient of the left field. The heteorogeneous correlation map for the kth left field is $r[s(\mathbf{x}, t), a_k^w(t)]$, the correlation between the left field and the kth expansion coefficient of the right field. Corresponding definitions apply to correlation maps for the right field. Covariance maps are also defined in an analogous manner. The contribution of each mode to the overall covariance is conveniently measured in terms of the fraction of the squared covariance explained (section 2b of Bretherton et al. 1992).

APPENDIX B

Significance of Second Mode

A liberal quantitative estimate of the degree of separation between the second mode of covarying ASO

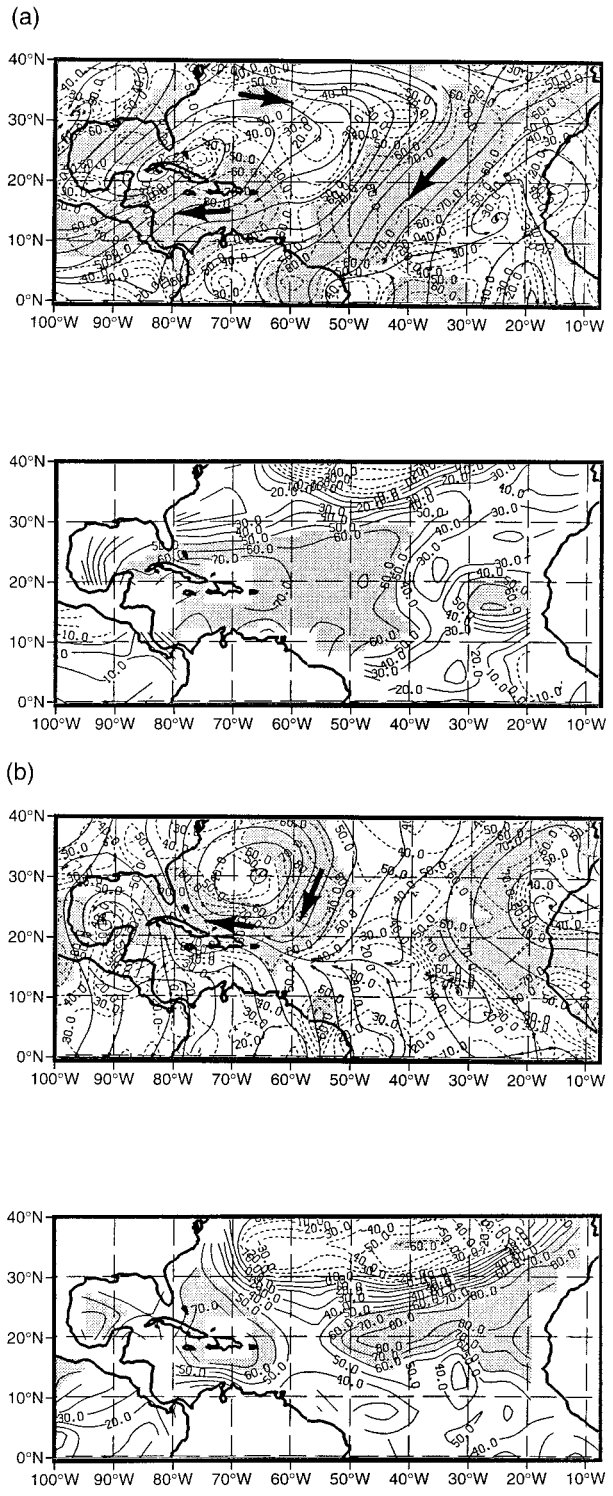

FIG. B1. Same as Fig. 8 but for (a) the first half of the period (1968–80) and (b) the second half (1981–92). Significance levels have been adjusted to account for the smaller sample sizes.

∇SST and ASO $\mathbf{V}_z$ variability and modes immediately adjacent can be made by assuming that the 25-yr series of winds and SSTs are serially uncorrelated. Then, applying the analysis of North et al. (1982) for EOFs to the SVDs [see discussion in section 4 of Cheng and Dunkerton (1995)], it is found that the second SVD mode is separated from the first (dominant) mode by 1.0 standard errors and from the third mode (which itself is not statistically significant) by 0.5 standard errors. By North et al.'s criterion, even these liberal values are too small to imply a clear statistical separation of the modes. Serial correlations within the series will decrease the number of degrees of freedom, thereby increasing the standard error and reducing the effective separation.

The statistical robustness of the second SVD mode has, however, been confirmed using an alternative method similar to that applied by Wallace et al. (1992), which is not dependent on the degree of serial correlation. The SVD analysis has been repeated on subsets of the data for the first of the period (1968–80) and second half (1981–92). The second modes derived from the first and second halves, shown in Fig. B1, show good qualitative agreement with the mode from the full record (Fig. 8). In particular, both halves evidence positive SST anomalies in the main development region that are associated with anticyclonic $\mathbf{V}_z$ anomalies in the northwestern part of the Atlantic basin. Unlike the Monte Carlo test, this test does not reorder the fields, so that serial correlations are retained. And, despite the pessimistic quantitative estimates using the criterion of North et al. (1982), the robustness of the character of the second mode supports the conclusion that it is not simply a result of random relationships. Also, both expansion coefficients for each half of the series are significantly correlated with hurricane frequency at the 80% level.

REFERENCES

Anthes, R. A., 1982: *Tropical Cyclones—Their Evolution, Structure and Effects. Meteor. Monogr.,* No. 19, Amer. Meteor. Soc., 208 pp.

Bretherton, C. S., C. Smith, and J. M. Wallace, 1992: An intercomparision of methods for finding coupled patterns in climate data. *J. Climate,* **5,** 541–560.

Carlson, T., 1971: An apparent relationship between sea-surface temperature of the tropical Atlantic and the development of African disturbances into tropical storms. *Mon. Wea. Rev.,* **99,** 309–310.

Chelton, D., 1983: Effects of sampling errors in statistical estimation. *Deep-Sea Res.,* **30,** 1083–1103.

Cheng, X., and T. J. Dunkerton, 1995: Orthogonal rotation of spatial patterns derived from singular value decomposition analysis. *J. Climate,* **8,** 2631–2643.

Davis, R., 1976: Predictability of sea surface temperature and sea level pressure anomalies over the North Pacific Ocean. *J. Phys. Oceanogr.,* **6,** 246–266.

——, 1977: Techniques for statistical analysis and prediction of geophysical fluid systems. *Geophys. Astrophys. Fluid Dyn.,* **8,** 245–277.

Folland, C., J. Owen, M. N. Ward, and A. Colman, 1991: Prediction of seasonal rainfall in the Sahel region using empirical and dynamical methods. *J. Forecasting,* **10,** 21–56.

Frank, N. L., 1970: Atlantic tropical systems of 1969. *Mon. Wea. Rev.*, **98,** 307–314.

Goldenberg, S. B., and L. J. Shapiro, 1996: Physical mechanisms for the association of El Niño and West African rainfall with Atlantic major hurricanes. *J. Climate,* **9,** 1169–1187.

Gray, W. M., 1968: Global view of the origin of tropical disturbances and storms. *Mon. Wea. Rev.,* **96,** 669–700.

——, 1984: Atlantic seasonal hurricane frequency. Part I: El Niño and 30 mb quasi-biennial oscillation influences. *Mon. Wea. Rev.,* **112,** 1649–1668.

——, 1990: Strong association between West African rainfall and U.S. landfall of intense hurricanes. *Science,* **249,** 1251–1256.

Horel, J. D., 1981: A rotated principal component analysis of the interannual variability of the Northern Hemisphere 500-mb height field. *Mon. Wea. Rev.,* **109,** 2080–2092.

Kleinbaum, D., and L. Kupper, 1978: *Applied Regression Analysis and Other Multivariable Methods.* Duxbury Press, 556 pp.

Landsea, C. W., 1993: The climatology of intense (or major) Atlantic hurricanes. *Mon. Wea. Rev.,* **121,** 1703–1713.

——, and W. M. Gray, 1992: The strong association between western Sahelian monsoon rainfall and intense Atlantic hurricanes. *J. Climate,* **5,** 1528–1534.

——, ——, G. D. Bell, and S. B. Goldenberg, 1998: The extremely active 1995 Atlantic hurricane season: Environmental conditions and verification of seasonal forecasts. *Mon. Wea. Rev.,* **126,** 1174–1193.

Lorenz, E., 1956: Empirical orthogonal functions and statistical weather prediction. Statistical Forecasting Project Rep. 1, Dept. of Meteorology, Massachusetts Institute of Technology, 49 pp. [NTIS AD-110-268.]

North, G., T. Bell, R. Cahalan, and F. Moeng, 1982: Sampling errors in the estimation of empirical orthogonal functions. *Mon. Wea. Rev.,* **110,** 699–706.

Oort, A. H., Y. H. Pan, R. W. Reynolds, and C. F. Ropelewski, 1987: Historical trends in the surface temperature over the oceans based on the COADS. *Climate Dyn.,* **2,** 29–38.

Ooyama, K. V., 1987: Scale-controlled objective analysis. *Mon. Wea. Rev.,* **115,** 2479–2506.

Palmén, E., 1948: On the formation and structure of tropical hurricanes. *Geophysica,* **3,** 26–38.

Prohaska, J., 1976: A technique for analyzing the linear relationships between two meteorological fields. *Mon. Wea. Rev.,* **104,** 1345–1353.

Raper, S. C. B., 1993: Observational data on the relationships between climatic change and the frequency and magnitude of severe tropical storms. *Climate and Sea Level Change: Observations, Projections and Implications,* R. A. Warrick, E. M. Barrow, and T. M. L. Wigley, Eds., Cambridge University Press, 192–212.

Richman, M. B., 1986: Rotation of principal components. *J. Climatol.,* **6,** 293–335.

Shapiro, L. J., 1982: Hurricane climatic fluctuations. Part II: Relation to large-scale circulation. *Mon. Wea. Rev.,* **110,** 1007–1013.

——, 1984: Sampling errors in statistical models of tropical cyclone motion: A comparison of predictor screening and EOF techniques. *Mon. Wea. Rev.,* **112,** 1378–1388.

——, 1986: The three-dimensional structure of synoptic-scale disturbances over the tropical Atlantic. *Mon. Wea. Rev.,* **114,** 1876–1891.

——, 1987: Month-to-month variability of the Atlantic tropical circulation and its relationship to tropical storm formation. *Mon. Wea. Rev.,* **115,** 2598–2614.

Siegel, S., 1956: *Nonparametric Statistics.* McGraw-Hill, 312 pp.

Wallace, J. M., C. Smith, and C. S. Bretherton, 1992: Singular value decomposition of wintertime sea surface temperature and 500-mb height anomalies. *J. Climate,* **5,** 561–576.